Published in final edited form as:
J Nat Prod. 2013 June 28; 76(6): 1175–1181. doi:10.1021/np400320r.

Inducers of Hypoxic Response: Marine Sesquiterpene Quinones Activate HIF-1

Lin Du[†,§], **Yu-Dong Zhou**[†,*], and **Dale G. Nagle**[†,‡,*]

[†]Department of Pharmacognosy, University of Mississippi, University, Mississippi 38677, United States

[‡]Research Institute of Pharmaceutical Sciences, School of Pharmacy, University of Mississippi, University, Mississippi 38677, United States

Abstract

The hypoxia-inducible factor-1 (HIF-1) transcription factor regulates cellular oxygen homeostasis. Agents that activate HIF-1 and downstream HIF targets represent potential drug leads for the prevention and/or treatment of ischemic disorders. In a search for small-molecule HIF-1 activators, 1936 marine invertebrate and algal extract samples (U.S. National Cancer Institute's Open Repository) were evaluated for HIF-1 activation activity in a cell-based reporter assay. Bioassay-guided fractionation of two active extracts of the sponge *Dactylospongia elegans* afforded four new sesquiterpene quinones (**2**–**5**), one new sesquiterpene phenol (**6**), the known Golgi disruptor ilimaquinone (**1**), and three previously reported ilimaquinone analogues (**7**–**9**). While antiproliferative activity was observed at higher concentrations, the sesquiterpene quinones (**1**–**3**) possessing a 2-hydroxy-5-methoxy-1,4-benzoquinone moiety activated HIF-1 and increased the expression of HIF-1 target gene vascular endothelial growth factor (VEGF) in T47D cells.

The transcription factor hypoxia-inducible factor (HIF) triggers various adaptive responses to hypoxic conditions (decreased oxygen tension) by transactivating a myriad of genes.[1] HIF is a heterodimer of an oxygen-labile α subunit and a constitutively expressed β subunit, with both being members of the basic helix-loop-helix PER-ARNT-SIM (bHLH-PAS) family.[2] There are three major HIFα isoforms in humans: HIF-1α, HIF-2α, and HIF-3α.[3] Expressed in all metazoan species examined, the founding member HIF-1 controls oxygen homeostasis by regulating the expression of hundreds of genes.[1,3] Apart from hypoxia, HIF-1 can be activated by non-hypoxic stimuli that range from transition metals, iron chelators, genetic alterations (e.g., activation of oncogenes, and inactivation of tumor suppressor genes.), lipopolysaccharides (LPS), thrombin, to angiotensin II (Ang II).[4] Natural product-based HIF-1 activators include alkaloids, phenolic compounds, terpenoids/steroids, and carbohydrates.[5] Therapeutically, small-molecule HIF-1 activators could be explored as new treatment options for ischemia/hypoxia-related diseases.[1,5]

In a campaign to discover novel natural product-derived HIF-1 activators, lipid extracts of the sponge *Dactylospongia elegans* Thiele (Thorectidae) activated HIF-1 in a cell-based reporter assay.[6] Bioassay-guided isolation and structure elucidation of the active extracts

[*]Corresponding Author: Tel: (662) 915-7026. Fax: (662) 915-6975. dnagle@olemiss.edu (D.G.N.). Tel: (662) 915-7026. Fax: (662) 915-6975. ydzhou@olemiss.edu (Y.-D.Z.).
[§]**Present Address:** Natural Products Discovery Group, Department of Chemistry and Biochemistry, Stephenson Life Sciences Research Center, 101 Stephenson Parkway, Room 1000, University of Oklahoma, Norman, OK 73019-5251 U.S.A.

The authors declare no competing financial interest.

Supporting Information. NMR spectra for **2**–**6** and compound purities. This material is available free of charge via the Internet at http://pubs.acs.org.

afforded the known sesquiterpene quinone ilimaquinone (**1**),[7,8] four new ilimaquinone analogues (**2**–**5**), one new sesquiterpene phenol (**6**), and three known analogues 8-*epi*-*ent*-chromazonarol (**7**),[9] cyclospongiaquinone-1 (**8**),[10,11] and cyclospongiaquinone-2 (**9**).[10,11] Sesquiterpene quinones and hydroquinones are relatively common marine natural products that have been isolated from various sponge families (e.g., Dysideidae, Thorectidae, Spongiidae, and Haploscleridae). These sesquiterpenes typically possess a drimane or 4,9-friedodrimane skeleton.[12] Many C_{15}-C_6 sesquiterpenes exhibit pronounced cytotoxic/antitumor,[13,14] antimicrobial,[15] and anti-HIV activities.[16] Herein, the isolation, structure elucidation, and HIF-1 activation-associated activities of **1**–**9** are described.

RESULTS AND DISCUSSION

In a human breast tumor T47D cell-based reporter assay,[6] extract samples of the sponge *Dactylospongia elegans* Thiele (Thorectidae) activated HIF-1 by 426% (NIH collection no. C028903, 10 μg mL^{-1}) and 452% (NIH collection no. C030171, 10 μg mL^{-1}), respectively. Bioassay-guided isolation and structure elucidation of the extract sample C028903 (3.0 g) afforded one major compound, the known sesquiterpene quinone ilimaquinone (**1**).[7,8] Similar isolation efforts of the extract sample C030171 (3.0 g) yielded five new compounds (**2**–**6**), and three known compounds (**7**–**9**).

Compound **2** was obtained as an optically active yellow amorphous solid. Its molecular formula, $C_{22}H_{30}O_4$, was established on the basis of its HRESIMS data (index of hydrogen deficiency = 8). The IR and UV spectra suggested the presence of a 1,4-benzoquinone chromophore (IR: 1645 and 1608 cm^{-1}; UV: λ_{max} 287 nm). The ^{13}C NMR and DEPT spectra demonstrated the presence of 22 carbons, accounting for four methyls, six sp^3 methylenes, one sp^2 methylene, two sp^3 methines, one sp^2 methine, two sp^3 quaternary carbons, and six sp^2 quaternary carbons. The ^1H and ^{13}C NMR spectra (Tables 1 and 2) suggested the presence of a dioxygenated-1,4-benzoquinone moiety [δ_H 5.79 (1H, s); δ_C 102.1 (CH), 118.7 (C), 152.8 (C), 161.3 (C), 182.6 (C), 182.6 (C)], an exomethylene [δ_H 4.68 (1H, s), 4.61 (1H, s); δ_C 105.8 (CH_2), 152.8 (C)], a methoxy [δ_H 3.80 (3H, s); δ_C 56.8 (CH_3)], and three methyl groups [δ_H 0.82 (3H, s), 1.02 (3H, d, J = 6.7 Hz), 1.19 (3H, s); δ_C 15.9 (CH_3), 24.7 (CH_3), 31.2 (CH_3)]. The methoxy group was connected to C-20 on the benzoquinone moiety based on the observed HMBC correlation from -OMe (δ_H 0.82) to C-20 (Figure 1). The structure of **2** was deduced to contain a 4,9-friedodrimane-type sesquiterpene moiety based on the following correlations in the HMBC spectrum: H-3/C-1, C-2; H-6/C-7, C-8; H-10/C-1, C-2; H-11/C-3, C-4; Me-12/C-4, C-5, C-6, C-10; Me-13/C-7, C-8, C-9; and Me-14/C-8, C-9, C-10, C-15 (Figure 1). The benzoquinone and sesquiterpene moieties were connected between C-15 and C-16 from the key HMBC correlations between H-15 to C-16, C-17, and C-21 (Figure 1). This sesquiterpene assemblage suggested that **2** is a new stereoisomer of ilimaquinone (**1**)[7,8] and 5-*epi*-ilimaquinone.[9,17] The relative configuration of **2** was established from the following NOESY correlations: Me-12/H-10, H-15a (δ_H 2.65); Me-14/H-8, 2H-1; and H-15b (δ_H 2.40)/Me-13 (Figure 2). Thus, **2** was shown to be a C-8 epimer of 5-*epi*-ilimaquinone that was assigned as 5,8-*diepi*-ilimaquinone.[9, 17]

The molecular formula of **3** was established as $C_{22}H_{30}O_4$ on the basis of the HRESIMS data. As in the structure of **2**, the ^1H and ^{13}C NMR spectra showed diagnostic resonances for the same 1,4-benzoquinone-type moiety [δ_H 3.84 (3H, s), 5.83 (1H, s), 7.84 (1H, s); δ_C 102.0 (CH), 118.7 (C), 152.9 (C), 161.7 (C), 182.5 (C), 182.6 (C)] (Tables 1 and 2). In the sesquiterpene portion of the molecule, the ^{13}C NMR data indicated the presence of three methyls, seven methylene, two methines, and three quaternary carbons (Table 2). The ^1H NMR and ^{13}C NMR resonances were similar to those of **2**, except that the resonances of the C-5–C-11 exomethylene moiety was replaced by an isolated AB system [δ_H 0.52 (1H, d, J =

4.0 Hz) and 0.03 (1H, d, J = 4.0 Hz)/δ_C 24.9] that was characteristic of a cyclopropyl ring system (Tables 1 and 2). Two remaining cyclopropyl carbons (δ_C 17.7 and 26.3) were deduced from their correlations with adjacent cyclopropyl protons observed in the HMBC spectrum (Figure 1). The spectra were not identical, but correlations observed in the 2D-NMR datasets acquired for **3** matched those observed for the known compound dactylospongiaquinone,[10] indicating that both are epimers with the same planar structure. The relative configuration of **3** was explored by analysis of the NOESY data (Figure 2). Strong NOESY correlations between H-15a (δ_H 2.66)/Me-14/H-8, and those observed between H-15b (δ_H 2.35)/H-10/Me-13 indicated that C-15, Me-13, and H-10 have the same spatial order with respect to ring B. Further, key NOESY correlations between a cyclopropyl proton (δ_H 0.52) and H-1a (δ_H 0.80) and Me-14 are only possible with a *trans*-ring fused configuration. Thus, **3** was deduced to be a cyclopropyl-inverted analogue of dactylospongiaquinone that was assigned as 4,5-*diepi*-dactylospongiaquinone.

Compound **4** was isolated as a yellow amorphous solid and deduced to have the molecular formula $C_{22}H_{28}O_4$ by HRESIMS. Comparison of the ^1H and ^{13}C NMR spectra of **4** (Tables 1 and 2) with those of **2** indicated that both compounds possess 1,4-benzoquinone and sesquiterpenoid moieties, except that C-10 is replaced by an oxygenated quaternary carbon (δ_C 88.5). Key HMBC correlations between Me-12/Me-14/2H-15 and C-10 (Figure 1), and an additional degree of hydrogen deficiency (relative to that of **2**) indicated that the 4,9-friedodrimane skeleton to be connected to the dialkoxy-1,4-benzoquinone through a C-10–O–C-17 bridge. The presence of a dihydropyran moiety was suggested by the corresponding loss of the hydroxy group absorption in the IR spectrum. The planar structure of **4** was thus determined to be that of a new epimer of the two previously reported compounds dactyloquinones A and B.[18] The relative configuration of **4** was determined from the following NOESY correlations (Figure 2): H-15a (δ_H 2.58) to Me-12 and Me-13; Me-14 to H-8 and H-15b (δ_H 2.04); and H-15b to Me-13. Thus, the structure of **4** was deduced to be the C-8-epimer of dactyloquinone B and has been assigned the trivial name 8-*epi*-dactyloquinone B.[18]

Compound **5** was purified as a yellow amorphous solid with the same molecular formula as **4** ($C_{22}H_{28}O_4$) by HRESIMS. Similarities in the 1D- and 2D-NMR data (Tables 1 and 2) with those of **3** and **4** suggested that the planar structure of **5** is an analogue of **3** with a dihydropyran ring. The relative configuration of **5** was deduced from the following NOESY correlations (Figure 2): H-15a (δ_H 2.30) to H-8 and Me-13; H-15b (δ_H 2.19) to H-1a (δ_H 1.50); H-12a (δ_H 0.65) to H-1b (δ_H 1.26) and Me-14; and H-8 to Me-14. Thus, **5** was assigned as 10,17-*O*-cyclo-4,5-*diepi*-dactylospongiaquinone.

The molecular formula of **6** was established as $C_{23}H_{32}O_5$ by HRESIMS. The ^{13}C NMR spectrum contained diagnostic resonances for a penta-substituted phenyl group [δ_C 104.6 (C), 116.0 (CH), 120.4 (C), 128.1 (C), 150.4 (C), 151.9 (C)], a methoxy carbon at δ_C 52.1, and an acyl carbon at δ_C 171.0 (Table 2); the corresponding ^1H NMR spectrum ($CDCl_3$) exhibited a sole phenyl proton resonance at δ_H 7.15, a methoxy group at δ_H 3.88, and two exchangeable hydroxy protons at δ_H 5.45 and 11.06 (Table 1). The phenyl ring substitution pattern was deduced by the following HMBC correlations (Figure 1): H-15a and H-15b to C-16, C-17, and C-21; H-17 to C-15, C-19, C-21, and C-22; OH-19 to C-18, C-19, and C-20; and Me-23 to C-22. The remaining ^1H and ^{13}C NMR resonances of the sesquiterpene moiety were nearly identical to those observed in the spectra of cyclospongiaquinone-2 (**9**).[10] The quaternary carbon at δ_C 99.6 was indicative of a C-9 oxaspiro center, as in **9**. The high degree of similarity between their ^1H and ^{13}C NMR spectra indicated that **6** and **9** possess the same oxaspirocyclic architecture and sesquiterpene relative configurations. This was confirmed by HMBC (Figure 1) and NOESY (Figure 2) correlations. In **6**, strong HMBC couplings between Me-14 and C-1, C-5, C-9, and C-10 supported assignment of the

Me-14 substituent to the C-10 position, rather than at C-9. The key NOESY correlations between H-15a (δ_H 2.78) and H-8, and between H-15b (δ_H 3.50) and H-1a (δ_H 1.10)/H-5, indicated that **6** contains a *trans*-A,B-ring junction and that C-15, H-8, and H-5 are of the same orientation on ring B. As an apparent analogue of **9**, compound **6** was assigned the trivial name cyclospongiacatechol.

Concentration-response studies were performed to determine the effects of **1–9** on HIF-1 activity in a T47D cell-based reporter assay (Figure 3). An iron chelator, 1,10-phenanthroline, was included as a HIF-1 activator control.[6] Compounds **1–3**, each possessing a 2-hydroxy-5-methoxy-1,4-benzoquinone moiety, activated HIF-1 at 10 and 30 μM. For **1–3**, a higher level of induction was observed at 10 μM (930%, 830%, and 1000%, respectively). None of the other related compounds exhibited a statistically significant increase in HIF-1 activity. These observations suggest that the 2-hydroxy-1,4-benzoquinone moiety appears to be the key pharmacophore for sesquiterpene quinones **1–3** to activate HIF-1. Further, the stereochemical differences between the structures of **1** and **2** do not appear to significantly influence their relative potencies.

The expression of HIF-1 target gene vascular endothelial growth factor (VEGF) was monitored as an example to determine the effects of sesquiterpene quinones on HIF-1 downstream targets. VEGF is a potent angiogenic factor that stimulates angiogenesis.[18] Compounds **1–3** (10 μM, 16 h) increased the levels of both secreted (Figure 4A) and cellular VEGF proteins in T47D cells (Figure 4B). This response is similar to that observed with the positive control 1,10-phenanthroline (10 μM).

To assess the impact of **1–9** treatment on cell proliferation/viability, concentration-response studies were performed in human breast tumor T47D and MDA-MB-231 cells (Figure 5). Concentration-dependent inhibition of cell proliferation/viability was observed following 48 h of compound treatment. Except for **7**, the compounds more effectively inhibited T47D cell proliferation (Figure 5A) relative to their effect on MDA-MB-231 cells (Figure 5B). At a concentration of 30 μM, compounds **1–3** suppressed T47D cell proliferation/viability by 56%, 60%, and 58%, respectively. The observation that certain ilimaquinone analogues inhibited cell proliferation/viability without HIF-inducing activity suggested that the pharmacophores responsible for these two bioactivities are not identical. In fact, cytotoxicity may account for the decrease in HIF-1 activation observed for higher concentrations of **1–3** (Figure 3).

Since Malhotra and coworkers discovered that ilimaquinone inhibits protein transport between successive Golgi cisternae by inducing the vesiculation of Golgi membranes,[19] ilimaquinone (**1**) has been used extensively as a chemical probe to investigate Golgi function and signaling pathways. Ilimaquinone triggers Golgi fragmentation in a manner that is reversible, energy-dependent, and independent of protein synthesis.[19] The Golgi fragmentation effect of ilimaquinone is mediated by membrane-bound heterotrimeric G proteins,[20] phospholipase D,[21] and protein kinase D.[22,23] In addition, ilimaquinone also depolymerizes microtubules.[24] The cellular targets of ilimaquinone were identified as *S*-adenosylmethionine synthetase, *S*-adenosylhomocysteinase, and methyl transferases by an affinity chromatography-based approach.[25] The disruption of subcellular organelles may contribute to the reported antiviral[26] and antitumor[27,28] activities attributed to ilimaquinone. In this study, ilimaquinone (**1**) and its two close analogues **2** and **3** were found to activate HIF-1 and stimulate the production of HIF-1 target VEGF proteins in both T47D and PC-3 cells (data not shown). The hydroxy group of the substituted 1,4-benzoquinone appears to be indispensable for the HIF-1 activation effects produced by **1–3**. Alteration of this hydroxy-1,4-benzoquinone unit by ring formation or its replacement with a phenol completely abrogated their activities. At this time, neither the role of the Golgi apparatus in

HIF-1 signaling nor the mechanism for ilimaquinone to activate HIF-1 has been elucidated. Mechanistic studies are underway to resolve the mechanism of action for ilimaquinone and related analogues to activate HIF-1. The underlying mechanisms of sesquiterpene quinones and their therapeutic potential for the treatment of ischemic diseases require further evaluation in biologically relevant systems.

EXPERIMENTAL SECTION

General Experimental Procedures

Optical rotations were obtained on an AP IV/589-546 digital polarimeter. A Bruker Tensor 27 Genesis Series FTIR was used to obtain the IR spectrum, and a Varian 50 Bio spectrophotometer was used to record the UV spectra. The NMR spectra were recorded in $CDCl_3$ on AMX-NMR spectrometers (Bruker) operating at 400 MHz for ^1H and 100 MHz for ^{13}C, respectively. Residual solvent resonances (δ 7.26 for ^1H and δ 77.16 for ^{13}C) were used as internal references for the NMR spectra recorded running gradients. The HRESIMS were determined on a Bruker Daltonic micro TOF fitted with an Agilent 1100 series HPLC and an electrospray ionization source. TLC was performed using Merck Si60F254 or Si60RP18F254 plates, sprayed with 10% H_2SO_4 in EtOH, visualized under UV light at 254 nm, and heated to char. The silica gel (32–63 μm) was from Selecto Scientific (Suwanee, GA, USA). HPLC was conducted on a Waters system, equipped with a 600 controller and a 996-photodiode array detector. Solvents (HPLC grade for HPLC, and reagent grade for extractions and column chromatography) were from Fisher Scientific unless otherwise specified. A semi-preparative HPLC column (Phenomenex Luna, C_{18}, 5 μm, 250 × 10.00 mm) was employed for isolation. Isocratic and gradient systems comprising MeCN and H_2O as solvents were used to generate optimal compound resolution. The purities of the compounds were judged on the percentage of the integrated signal at UV 220 nm. All purified compounds submitted for bioassay were at least 95% pure as determined by this method (Supporting Information).

Sponge Material

The sponge materials were obtained from the U.S. National Cancer Institute's Open Repository Program. *Dactylospongia elegans* was collected (collection no. 0CDN9429; NPID no. C028903) at a depth of 9 m off the coast of Malaysia (October 16, 2006). *Dactylospongia elegans* (collection no. 0CDN9995; NPID no. C030171) was collected at a depth of 33 m off the coast of Palau (July 20, 2009). Both samples were frozen at −20 °C and ground in a meat grinder. The *D. elegans* collection no. 0CDN9429 sponge materials were identified by Dr. Belinda Alvarez de Glasby of the Museum of the Northern Territories, Darwin, Australia. The *D. elegans* collection no. 0CDN9995 sponge materials were identified by Dr. Michelle Kelly of the National Institute of Water and Atmospheric Research Limited, Auckland, New Zealand. Voucher specimens were placed on file with the Department of Invertebrate Zoology, National Museum of Natural History, Smithsonian Institution, Washington, DC.

Extraction and Isolation

Ground *D. elegans* sponge samples were extracted with water. The residual samples were then lyophilized and extracted with 50% MeOH in CH_2Cl_2,[29] residual solvents were removed under vacuum, and the extracts were stored at −20 °C in the NCI repository at the Frederick Cancer Research and Development Center (Frederick, MD). The *D. elegans* extract (no. C028903, 3.0 g) was suspended with 50% MeOH in CH_2Cl_2 and the residue was removed by filtration. To reduce the loss of potential HIF-1 activity,[30] silica gel chromatography was specifically avoided in the bioassay-guided separation of the active constituents. The supernatant was dried under vacuum and passed over Diaion HP-20SS gel

with step gradients of MeOH in H_2O (30:70, 70:30, 90:10, 100:0) and 50% MeOH in $CHCl_3$. The fourth fraction (HIF-1 activation by 353%, 10 μg mL^{-1}, 1.04 g) was crystallized from MeOH to afford **1** (130 mg, 4.3% yield). A second *D. elegans* extract sample (no. C030171, 3.0 g) was similarly fractionated by passage over HP-20SS (40 g) with gradients of MeOH in H_2O (50:50, 70:30, 80:20, 85:15, 90:10, 95:5, 100:0) and 50% MeOH in $CHCl_3$. Fractionation of this second extract produced eight further fractions. Four fractions that eluted with 85% to 100% MeOH in H_2O (HIF-1 activation by 81% to 818%, 10 μg mL^{-1}) were combined (1.6 g) and separated by passage over Sephadex LH-20 (50% MeOH in $CHCl_3$) to obtain six subfractions. Two active subfractions (HIF-1 activation by 395% and 347%, respectively, 10 μg mL^{-1}) were combined (208 mg), passed through Sephadex LH-20 (100% MeOH), and subjected to HPLC (Luna 5 μm, ODS-3, 100 Å, 250 × 10.00 mm, isocratic 90% CH_3CN in H_2O, 4.0 mL min^{-1}) to produce **4** (3.0 mg, 0.10% yield), **5** (2.6 mg, 0.08% yield), **8** (34 mg, 1.13% yield), and **9** (10 mg, 0.33% yield). Guided by a similar UV-active TLC pattern, a relatively inactive fraction from the original LH-20 column (577 mg) was also passed over Sephadex LH-20 (100% MeOH) to produce four subfractions. A subfraction from the original LH-20 column that activated HIF-1 by 400% (10 μg mL^{-1}, 493 mg) was further separated by HPLC (Luna 5 μm, ODS-3, 100 Å, 250 × 10.00 mm, isocratic 90% CH_3CN in H_2O, 4.0 mL min^{-1}) to produce **2** (89 mg, 3.0% yield), **6** (28 mg, 0.93% yield), and a subfraction (120 mg) that was subjected to HPLC (Luna 5 μm, ODS-3, 100 Å, 250 × 10.00 mm, isocratic 82% CH_3CN in 0.1% TFA, 4.0 mL min^{-1}), to give **3** (34 mg, 1.1% yield) and **7** (70 mg, 2.3% yield).

Ilimaquinone (1)—yellow, amorphous solid; $[\alpha]^{24}_D$ −31.4 (*c* 0.14, $CHCl_3$); lit. $[\alpha]^{23}_D$ −23.2 (*c* 1.12, $CHCl_3$);[7] ^1H NMR and ^{13}C NMR data were consistent with previously published results;[7,8] HRESIMS *m*/*z* 357.2076 $[M-H]^-$ (calcd for $C_{22}H_{29}O_4$, 357.2071).

5,8-*Diepi*-ilimaquinone (2)—yellow, amorphous solid; $[\alpha]^{24}_D$ −10.6 (*c* 0.17, $CHCl_3$); UV (MeOH) λ_{max} (log ε) 206 (4.17), 287 (4.13) nm; IR (film) ν_{max} 3340, 2943, 1645, 1608, 1539, 1522, 1457, 1380, 1350, 1317, 1233, 1033, 974, 890, 842, 796 cm^{-1}; ^1H NMR ($CDCl_3$, 400 MHz) and ^{13}C NMR ($CDCl_3$, 100 MHz) data, see Tables 1 and 2; HRESIMS *m*/*z* 357.2073 $[M-H]^-$ (calcd for $C_{22}H_{29}O_4$, 357.2071).

4,5-*Diepi*-dactylospongiaquinone (3)—yellow, amorphous solid; $[\alpha]^{24}_D$ −2.4 (*c* 0.17, $CHCl_3$); UV (MeOH) λ_{max} (log ε) 205 (4.09), 286 (4.16) nm; IR (film) ν_{max} 3367, 2944, 1644, 1608, 1454, 1380, 1352, 1318, 1233, 1129, 1033, 842 cm^{-1}; ^1H NMR ($CDCl_3$, 400 MHz) and ^{13}C NMR ($CDCl_3$, 100 MHz) data, see Tables 1 and 2; HRESIMS *m*/*z* 357.2068 $[M-H]^-$ (calcd for $C_{22}H_{29}O_4$, 357.2071).

8-*Epi*-dactyloquinone B (4)—yellow, amorphous solid; $[\alpha]^{24}_D$ +136.5 (*c* 0.15, $CHCl_3$); UV (MeOH) λ_{max} (log ε) 203 (4.06), 288 (4.13) nm; IR (film) ν_{max} 2979, 2945, 1663, 1603, 1458, 1352, 1275, 1216, 1044, 943, 899 cm^{-1}; ^1H NMR ($CDCl_3$, 400 MHz) and ^{13}C NMR ($CDCl_3$, 100 MHz) data, see Tables 1 and 2; HRESIMS *m*/*z* 379.1900 [M+Na] (calcd for $C_{22}H_{28}O_4Na$, 379.1885).

10,17-*O*-Cyclo-4,5-*diepi*-dactylospongiaquinone (5)—yellow, amorphous solid; $[\alpha]^{24}_D$ −123.3 (*c* 0.12, $CHCl_3$); UV (MeOH) λ_{max} (log ε) 203 (3.96), 289 (4.09) nm; IR (film) ν_{max} 2942, 1662, 1601, 1460, 1385, 1351, 1264, 1240, 1209, 1153, 1084, 1042, 882, 843 cm^{-1}; ^1H NMR ($CDCl_3$, 400 MHz) and ^{13}C NMR ($CDCl_3$, 100 MHz) data, see Tables 1 and 2; HRESIMS *m*/*z* 379.1896 $[M+Na]^-$ (calcd for $C_{22}H_{28}O_4Na$, 379.1885).

Cyclospongiacatechol (6)—white, amorphous solid; $[\alpha]^{24}_D$ +9.7 (*c* 0.14, $CHCl_3$); UV (MeOH) λ_{max} (log ε) 219 (4.32), 283 (4.19) nm; IR (film) ν_{max} 3467, 3006, 2935, 1650,

1491, 1460, 1437, 1310, 1281, 1259, 1245, 1211, 1073, 1050, 1015, 982, 790, 715, 690 cm^{-1}; ^{1}H NMR ($CDCl_3$, 400 MHz) and ^{13}C NMR ($CDCl_3$, 100 MHz) data, see Tables 1 and 2; HRESIMS *m*/*z* 387.2178 $[M-H]^-$ (calcd for $C_{23}H_{31}O_5$, 387.2171).

Cell-Based Reporter and Proliferation/Viability Assays

Human breast tumor T47D and MDA-MB-231 cells (ATCC) were maintained in DMEM/F12 medium with L-glutamine (Mediatech), supplemented with fetal bovine serum [FBS, 10% (v/v), Hyclone] and a mixture of penicillin (50 units mL^{-1}) and streptomycin (50 μg mL^{-1}) (Lonza).

The cell-based reporter assay was performed as described with the pHRE3-TK-Luc construct to monitor HIF-1 activity.[6] For the cell proliferation/viability assay, plating of cells into 96-well plates, compound treatment (48 h), cell viability determination by the sulforhodamine B method, and data presentation were performed as described.[31]

ELISA Assay for Secreted VEGF Protein

The procedures were the same as previously described.[6] The levels of secreted and cellular VEGF proteins in T47D cell-conditioned medium and cell lysate samples were determined by ELISA, and normalized to the amount of cellular proteins quantified using a micro BCA assay kit (Thermo Fisher Scientific, Rockford, IL).

Statistical Analysis

Data comparison was performed with one-way ANOVA followed by Bonferroni post hoc analyses using GraphPad Prism 4. Differences between datasets were considered statistically significant when $p < 0.05$.

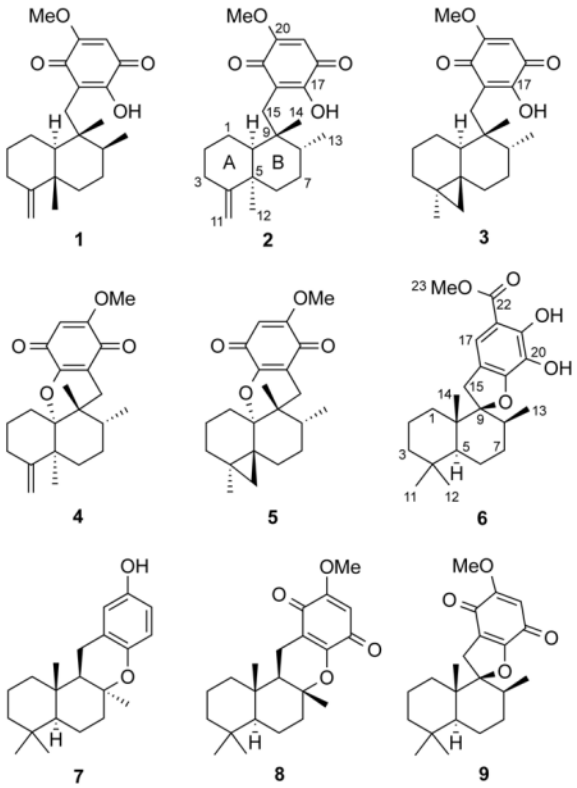

Supplementary Material

Refer to Web version on PubMed Central for supplementary material.

Acknowledgments

The authors thank the Natural Products Branch Repository Program at the National Cancer Institute for providing marine extracts from the NCI Open Repository used in these studies, Dr. D. J. Newman and E. C. Brown (NCI, Frederick, MD) for assistance with sample logistics and collection information, and Dr. S. L. McKnight (University of Texas Southwestern Medical Center at Dallas) for providing the pTK-HRE3-luc construct. This work was supported in part by the National Institutes of Health National Cancer Institute (grant CA98787), and the National Oceanic and Atmospheric Administration National Institute for Undersea Science and Technology (grant NA16RU1496). This investigation was conducted in a facility constructed with Research Facilities Improvement Grant C06 RR-14503-01 from the National Institutes of Health.

References

1. Semenza GL. Cell. 2012; 148:399–408. [PubMed: 22304911]
2. Semenza GL, Wang GL. J Biol Chem. 1995; 270:1230–1237. [PubMed: 7836384]
3. Greer SN, Metcalf JL, Wang Y, Ohh M. EMBO J. 2012; 31:2448–2460. [PubMed: 22562152]
4. Kuschel A, Simon P, Tug S. J Cell Physiol. 2012; 227:514–524. [PubMed: 21503885]
5. Nagle DG, Zhou YD. Curr Pharm Des. 2006; 12:2673–2688. [PubMed: 16842166]
6. Hodges TW, Hossain CF, Kim YP, Zhou YD, Nagle DG. J Nat Prod. 2004; 67:767–771. [PubMed: 15165135]
7. Luibrand RT, Erdman TR, Vollmer JJ, Scheuer PJ. Tetrahedron. 1979; 35:609–612.
8. Capon RJ, MacLeod JK. J Org Chem. 1987; 52:5059–5060.
9. Rodriguez J, Quinoa E, Riguera R, Peters BM, Abrell LM, Crews P. Tetrahedron. 1992; 48:6667–6680.
10. Jankam A, Somerville MJ, Hooper JNA, Brecknell DJ, Suksamrarn A, Garson MJ. Tetrahedron. 2007; 63:1577–1582.
11. Kazlauskas R, Murphy PT, Warren RG, Wells RJ, Blount JF. Aust J Chem. 1978; 31:2685–2697.
12. Blunt JW, Copp BR, Munro MHG, Northcote PT, Prinsep MR. Nat Prod Rep. 2010; 27:165–237. [PubMed: 20111802] and previous reviews in this series; Gordaliza M. Mar Drugs. 2010; 8:2849–2870. [PubMed: 21339953]
13. Muller WEG, Maidhof A, Zahn RK, Schroder HC, Gasiæ MJ, Heidemann D, Bernd A, Kurelec B, Eich E, Seibert G. Cancer Res. 1985; 45:4822–4826. [PubMed: 3839712]
14. Hsieh PW, Shen YC. J Nat Prod. 1997; 60:93–97. [PubMed: 9051909]
15. Rosa SD, Giulio AD, Iodice C. J Nat Prod. 1994; 57:1711–1716. [PubMed: 7714539]
16. Sarin PS, Sun D, Thornton A, Muller WEG. J Nat Cancer Inst. 1987; 78:663–666. [PubMed: 2435942]
17. Carte B, Rose CB, Faulkner DJ. J Org Chem. 1985; 50:2785–2787.
18. Chung AS, Ferrara N. Annu Rev Cell Dev Biol. 2011; 27:563–584. [PubMed: 21756109]
19. Takizawa PA, Yucel JK, Veit B, Faulkner DJ, Deerinck T, Soto G, Ellisman M, Malhotra V. Cell. 1993; 73:1079–1090. [PubMed: 8513494]
20. Jamora C, Takizawa PA, Zaarour RF, Denesvre C, Faulkner DJ, Malhotra V. Cell. 1997; 91:617–626. [PubMed: 9393855]
21. Sonoda H, Okada T, Jahangeer S, Nakamura S. J Biol Chem. 2007; 282:34085–34092. [PubMed: 17897952]
22. Jamora C, Yamanouye N, Van Lint J, Laudenslager J, Vandenheede JR, Faulkner DJ, Malhotra V. Cell. 1999; 98:59–68. [PubMed: 10412981]
23. Liljedahl M, Maeda Y, Colanzi A, Ayala I, Van Lint J, Malhotra V. Cell. 2001; 104:409–420. [PubMed: 11239398]
24. Veit B, Yucel JK, Malhotra V. J Cell Biol. 1993; 122:1197–1206. [PubMed: 8104190]

25. Radeke HS, Digits CA, Casaubon RL, Snapper ML. Chem Biol. 1999; 6:639–647. [PubMed: 10467129]
26. Loya S, Hizi A. J Biol Chem. 1993; 268:9323–9328. [PubMed: 7683648]
27. Liu H, Wang G, Namikoshi M, Kobayashi H, Yao X, Cai G. Pharm Biol. 2006; 44:522–527.
28. Lu PH, Chueh SC, Kung FL, Pan SL, Shen YC, Guh JH. Eur J Pharmacol. 2007; 556:45–54. [PubMed: 17140562]
29. McCloud TC. Molecules. 2010; 15:4526–4563. [PubMed: 20657375]
30. Datta S, Zhou YD, Nagle DG. J Nat Prod. 2013; 76:642–647. [PubMed: 23441686]
31. Liu Y, Veena CK, Morgan JB, Mohammed KA, Jekabsons MB, Nagle DG, Zhou YD. J Biol Chem. 2009; 284:5859–5868. [PubMed: 19091749]

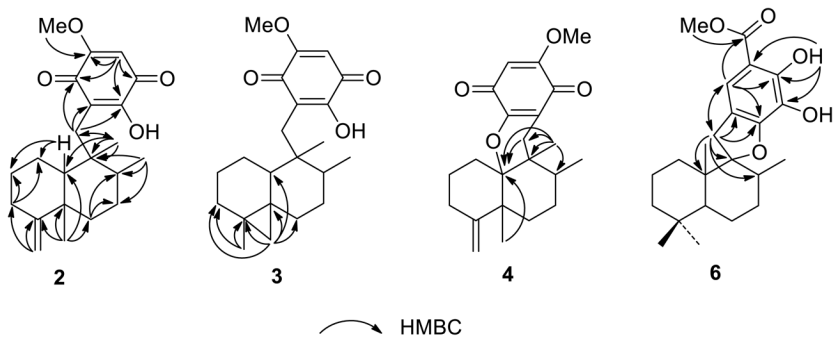

Figure 1.
Selected HMBC correlations of **2**–**4** and **6**.

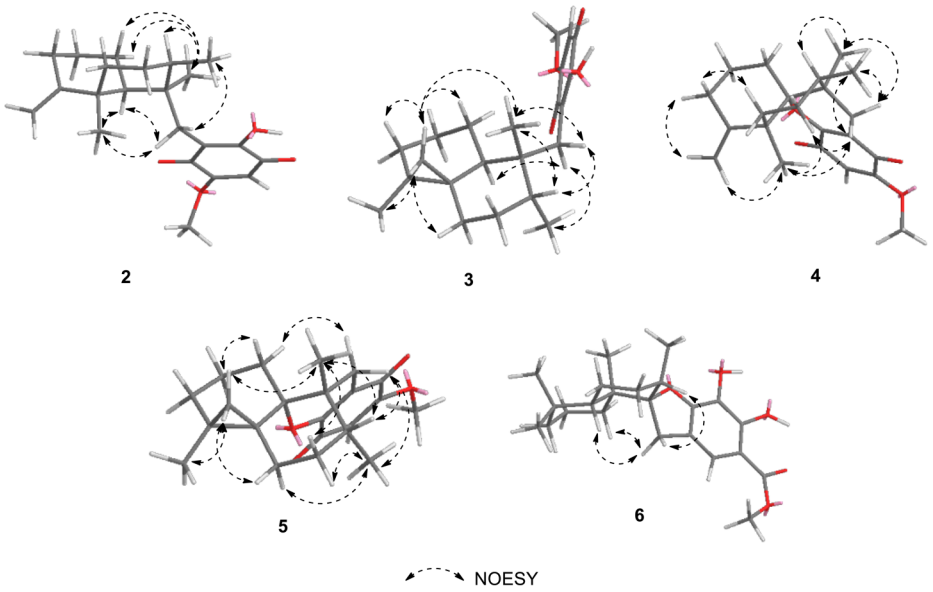

Figure 2.
Selected NOESY correlations of **2**–**6**.

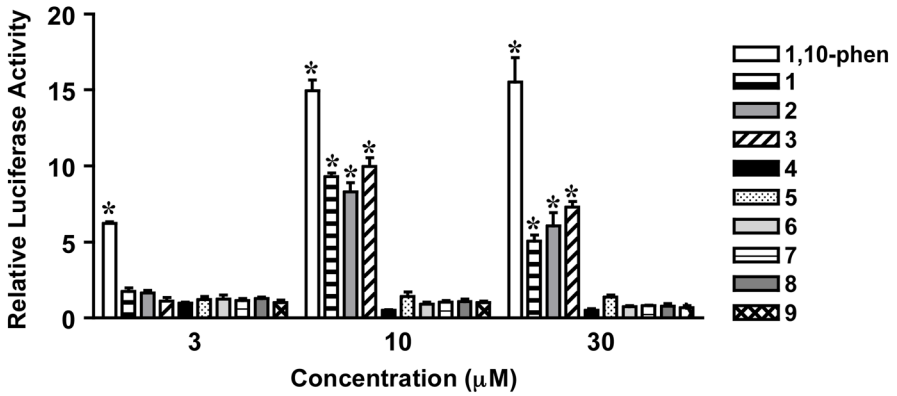

Figure 3.

Concentration-response results of **1**–**9** in a T47D cell-based reporter assay for HIF-1 activity. The compound 1,10-phenanthroline (1,10-phen) was used as a positive control. T47D cells transfected with the pHRE-luc construct were exposed to compounds at the specified concentrations for 16 h. Luciferase activity was normalized to that of the untreated control and presented as "Relative Luciferase Activity." Data shown are average + standard deviation ($n = 4$). An asterisk (*) indicates $p < 0.05$ when compared to the untreated control.

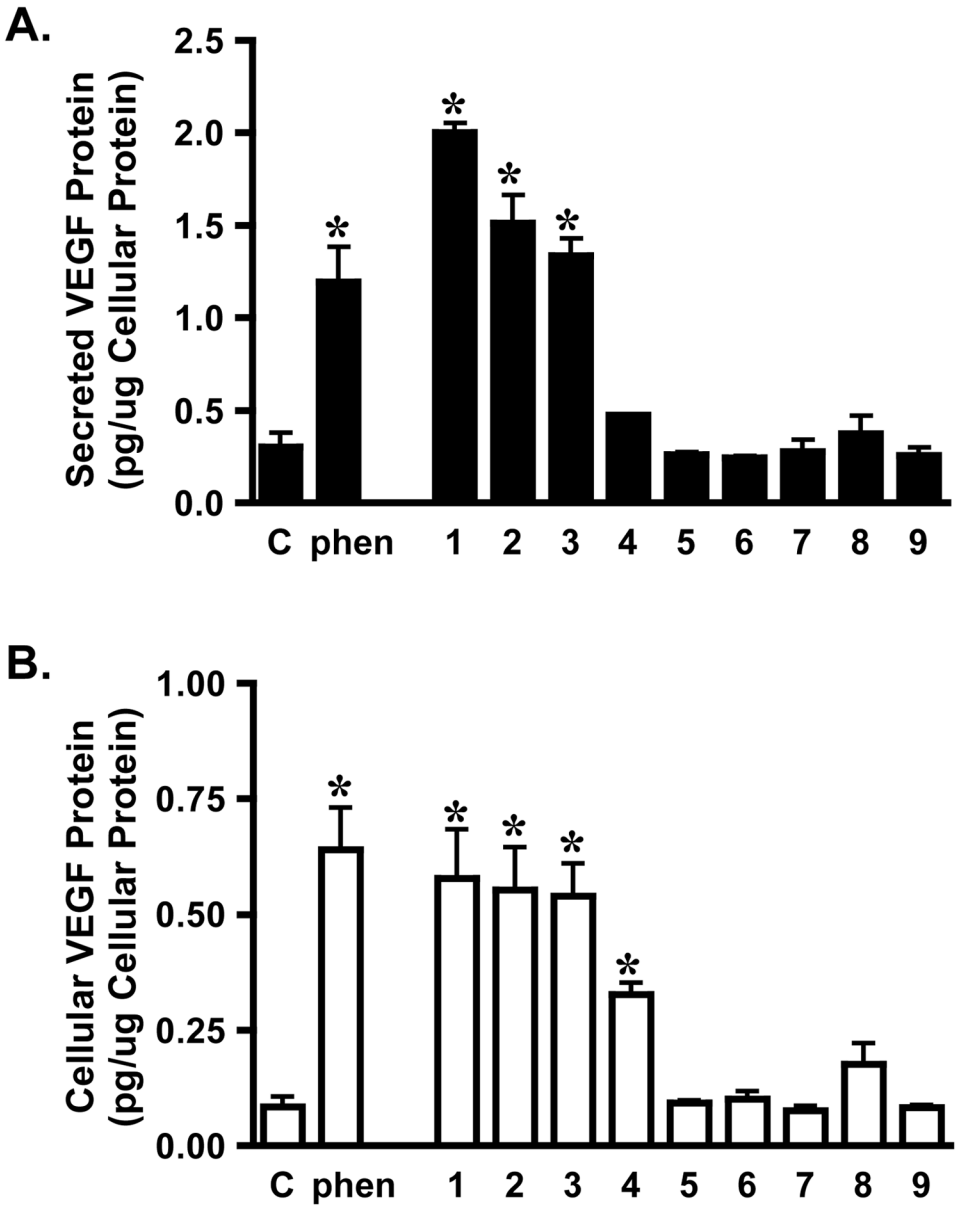

Figure 4.

Effects of **1**–**9** on VEGF protein expression. T47D cells were exposed to **1**–**9** and 1,10-phenanthroline (phen) as specified at the concentration of 10 μM for 16 h. The levels of secreted (A) and cellular VEGF proteins (B) were determined by ELISA and normalized to the quantity of cellular proteins. “C” represents untreated medium control. Data shown are average + standard deviation, pooled from two independent experiments ($n = 3$). An asterisk (*) indicates $p < 0.05$ when compared to the untreated control.

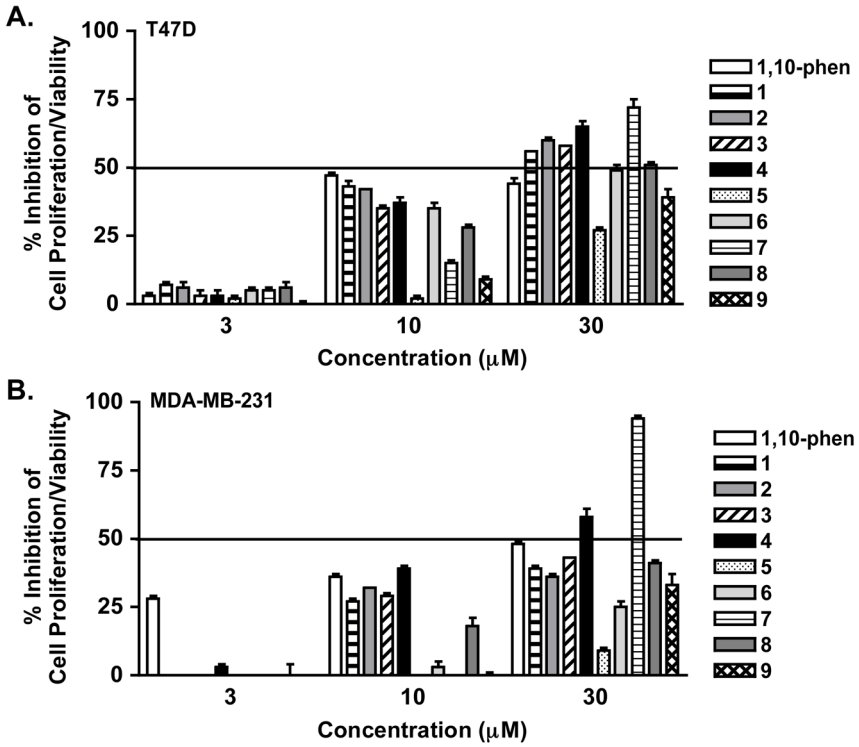

Figure 5.

Effects of **1–9** on cell proliferation/viability. T47D (A) and MDA-MB-231 cells (B) were exposed to **1–9** and 1,10-phenanthroline (1,10-phen) at the specified concentrations for 48 h. Cell viability was determined by the SRB method and presented as "% Inhibition" of the untreated control. Data shown are averages from one representative experiment performed in triplicate and the bars represent standard deviations.

Table 1

^{1}H NMR Spectroscopic Data for **2**–**6** (400 MHz, $CDCl_3$, δ ppm, J in Hz)[a,b]

number	2	3	4	5	6
1	1.79, m 1.60, m	1.56, m 0.80, m	2.04, m 1.96, m	1.50, m 1.26, m	1.25, m 1.10, m
2	1.79, m 1.44, m	1.46, m 1.25, m	2.00, m 1.71, m	1.50, m 1.20, m	1.59, m 1.24, m
3	2.29, m 2.09, m	1.56, m	2.36, m 2.25, m	1.84, m 1.66, m	1.34, m 1.09, m
5					1.00, m
6	1.81, m 1.44, m	1.83, m 0.92, m	2.12, m 1.15, m	2.19, m 0.93, m	1.52, m 1.47, m
7	1.79, m 1.19, m	1.80, m 1.17, m	1.55, m 1.51, m	2.04, m 1.37, m	1.62, m
8	1.44, m	1.53, m	1.87, m	1.66, m	2.04, m
10	1.67, m	1.79, m			
11	4.68, s 4.61, s	1.00, s	4.82, s 4.70, s	1.17, s	0.88, s
12	1.19, s	0.52, d, (4.0) 0.03, d, (4.0)	1.15, s	0.65, d (4.2) 0.36, d (4.2)	0.86, s
13	1.02, d (6.7)	1.17, d (6.8)	1.00, d (6.8)	0.91, d (7.3)	1.21, d[c]
14	0.82, s	0.89, s	0.95, s	1.20, s	1.22, s[c]
15	2.65, d (13.2) 2.40, d (13.2)	2.66, d (13.2) 2.35, d (13.2)	2.58, d (18.8) 2.04, d (18.8)	2.30, d (19.1) 2.19, d (19.2)	3.50, d (15.8) 2.78, d (15.8)
17					7.15, s
19	5.79, s	5.83, s	5.73, s	5.73, s	
23					3.88, s
HO-17		7.48, s			
HO-19					11.06, s
HO-20					5.45, br s
CH_3O-20	3.80, s	3.84, s	3.80, s	3.80, s	

[a] Assignments based on HSQC.

[b] All spectra recorded in $CDCl_3$.

[c] Resonances overlapped.

Table 2

^{13}C NMR Data of **2**–**6** (100 MHz, $CDCl_3$, δ ppm)[a,b]

number	2	3	4	5	6
1	22.6, CH_2	20.8, CH_2	30.9, CH_2	24.2, CH_2	32.3, CH_2
2	25.3, CH_2	23.1, CH_2	23.2, CH_2	15.7, CH_2	17.2, CH_2
3	32.3, CH_2	31.9, CH_2	32.7, CH_2	29.1, CH_2	42.0, CH_2
4	152.8, C	17.7, C	154.2, C	20.4, C	33.2, C
5	40.2, C	26.3, C	46.6, C	28.2, C	49.5, CH
6	31.1, CH_2	27.8, CH_2	36.4, CH_2	23.0, CH_2	17.8, CH_2
7	26.4, CH_2	27.9, CH_2	27.6, CH_2	28.2, CH_2	29.8, CH_2
8	38.9, CH	37.8, CH	39.3, CH	41.4, CH	41.0, CH
9	42.3, C	43.2, C	39.0, C	37.7, C	99.6, C
10	46.7, CH	40.0, CH	88.5, C	87.6, C	43.5, C
11	105.8, CH_2	22.5, CH_3	110.1, CH_2	22.5, CH_3	33.7, CH_3
12	31.2, CH_3	24.9, CH_2	20.4, CH_3	26.2, CH_2	21.6, CH_3
13	15.9, CH_3	15.1, CH_3	16.0, CH_3	17.6, CH_3	17.1, CH_3
14	24.7, CH_3	20.7, CH_3	26.0, CH_3	27.7, CH_3	17.1, CH_3
15	29.7, CH_2	29.2, CH_2	27.6, CH_2	30.7, CH_2	39.6, CH_2
16	118.7, C	118.7, C	114.7, C	118.6, C	120.4, C
17	152.8, C	152.9, C	154.2, C	154.4, C	116.0, CH
18	182.6, C	182.5, C	181.7, C	181.6, C	104.6, C
19	102.1, CH	102.0, CH	104.8, CH	105.0, CH	150.4, C
20	161.3, C	161.7, C	159.5, C	159.5, C	128.1, C
21	182.6, C	182.6, C	181.1, C	181.1, C	151.9, C
22					171.0, C
23					52.1, CH_3
CH_3O-20	56.8, CH_3	56.9, CH_3	56.5, CH_3	56.5, CH_3	

[a]Carbon type based on HSQC.

[b]All spectra recordeed in $CDCl_3$.